Towards novel entangled carbon nanotube composite electrodes

Gordon G. Wallace
University of Wollongong, gwallace@uow.edu.au

P. Sherrell
University of Wollongong, pcs759@uow.edu.au

J. Chen
University of Wollongong, junc@uow.edu.au

A. Minett
University of Wollongong, aminett@uow.edu.au

Towards novel entangled carbon nanotube composite electrodes

Abstract

The commercialization of carbon nanotube electrodes is impeded by the lack of bulk processing techniques. One approach to overcome this impediment is the growth of macroscopic CNT composite architectures which do not require any extra processing. Unfortunately the fundamental growth mechanisms of these carbon composites is not currently understood. To probe this mechanism a systematic examination of the effect of certain growth parameters was undertaken. Within this paper we present the promising preliminary findings of this study revealing extremely complex relationships between variables during growth. We also present the performance of the produced architectures as capacitor electrodes and the further improvement of these electrodes by doping with metallic nanoparticles.

Keywords

carbon, nanotube, towards, novel, entangled, composite, electrodes

Disciplines

Life Sciences | Physical Sciences and Mathematics | Social and Behavioral Sciences

Publication Details

Towards Novel Entangled Carbon Nanotube Composite Electrodes

Authors: Sherrell, P[1]. Chen, J[1]. Wallace, G, G[1]. Minett, A, I[1].
Affiliations: [1]Intelligent Polymer Research Institute, ARC Centre of Excellence for Electromaterials Science, University of Wollongong, Wollongong, NSW, Australia, 2522
aminett@uow.edu.au

ABSTRACT

The commercialization of carbon nanotube electrodes is impeded by the lack of bulk processing techniques. One approach to overcome this impediment is the growth of macroscopic CNT composite architectures which do not require any extra processing. Unfortunately the fundamental growth mechanisms of these carbon composites is not currently understood. To probe this mechanism a systematic examination of the effect of certain growth parameters was undertaken. Within this paper we present the promising preliminary findings of this study revealing extremely complex relationships between variables during growth. We also present the performance of the produced architectures as capacitor electrodes and the further improvement of these electrodes by doping with metallic nanoparticles.

INTRODUCTION

Carbon nanotubes (CNTs) have been the subject of intense research in terms of novel electrode materials, primarily due to the high conductivities and surface area's attainable with CNT structures.[1-5] A key limitation for many CNT applications is laborious post-processing regimes required to generate a suitable structure. Recent developments in chemical vapor deposition (CVD) of CNTs has lead to numerous 3D CNT architectures that can be utilized 'as grown'.[6-9] Due to the catalytic requirements of many electrochemical devices, specifically lithium ion (Li-ion) batteries and fuel cells (FCs), the doping of CNTs with metallic and metal-oxide nanoparticles (NPs) is crucial to device applications of CNT electrodes.[5, 10-13] As such, there are numerous methods that have been developed to achieve the desired doping, including; microwave-assisted polyol;[14-17] electrochemical;[17-19] sonolysis [17, 20] and auto-reduction deposition.[17, 21] In spite of these recent achievements the goal of a commercially available CNT electrode has not been realized.

In this paper we present a novel, flexible, 3D CNT composite architecture that has great potential for a range of electrochemical devices

EXPERIMENT

Carbon Nanotube Growth

3D CNT scaffolds were produced in a 3 stage Atomate tube furnace (Figure 1) utilizing Iron (III) Tosylate as a pre-cursor catalyst and acetylene as the carbon source. Samples were prepared by spin casting 2%, 5% or 10%, Fe (III) Tosylate in ethanol onto 4x10cm quartz slides at 1000rpm. The slides were dried at $100^{o}C$ for 10min to remove excess solvent and to prevent catalyst agglomeration. Following drying, the sheets were placed into the furnace between 100 and 400mm from the gas inlet and sealed. Argon was introduced at a flow of 200mL/min with

the furnace held at 100°C for 30min to purge oxygen from the system. The Argon flow was kept constant throughout the CVD experiment as a carrier gas. Reduction of the catalyst was performed between 500-600°C at a flow rate of 10mL/min of H_2 gas. The temperature gradient was further increased to 800-900°C prior to the introduction of acetylene at 20mL/min. Deposition was then performed for varying periods of time ranging from 15 to 60 minutes.[9]
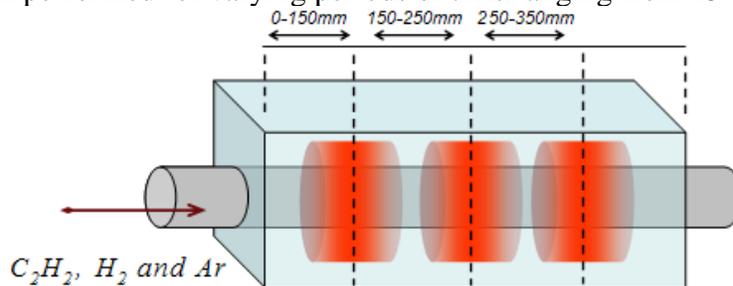
Figure 1. Schematic of the 3-Stage tube furnace utilized for the production of entangled carbon nanotube networks

Nanoparticle Deposition

Composite CNT/Metal NP electrodes were synthesized by a microwave-assisted polyol reduction method. The CNT scaffold was immersed in a solution of 20μL of 8% H_2PtCl_6 ($HAuCl_4$ or $PdCl_2.xH_2O$) (Sigma-Aldrich) in 10mL Ethylene Glycol (EG) and was exposed to 1200W microwave irradiation for 5second periods until reduction was observed to occur.

Carbon Nanotube Growth

Scanning electron microscopy was carried out on a Jeol 6460 with no conductive coating required for imaging. Electrochemical characterization, in the form of cyclic voltammograms (CVs), were tested in a conventional three electrode cell in 0.1M Tetrabutylammonium perchlorate in acetonitrile against an Ag/Ag^+ reference electrode. Capacitances were measured at 0V and power and energy densities were calculated from the cyclic voltammograms.

DISCUSSION

It is well know that CVD of CNTs is highly dependant on a range of variables, including carbon source gas, decomposition temperature, and growth time. Optimization of these parameters for entangled CNT (eCNT) composite architectures has not been examined in detail. Indeed it is theorized that these variables will have an even greater affect in eCNT systems due to the propensity of defects visible in the structure. Previously we have reported the large scale production of unoptimised 3D eCNT architectures.[9]
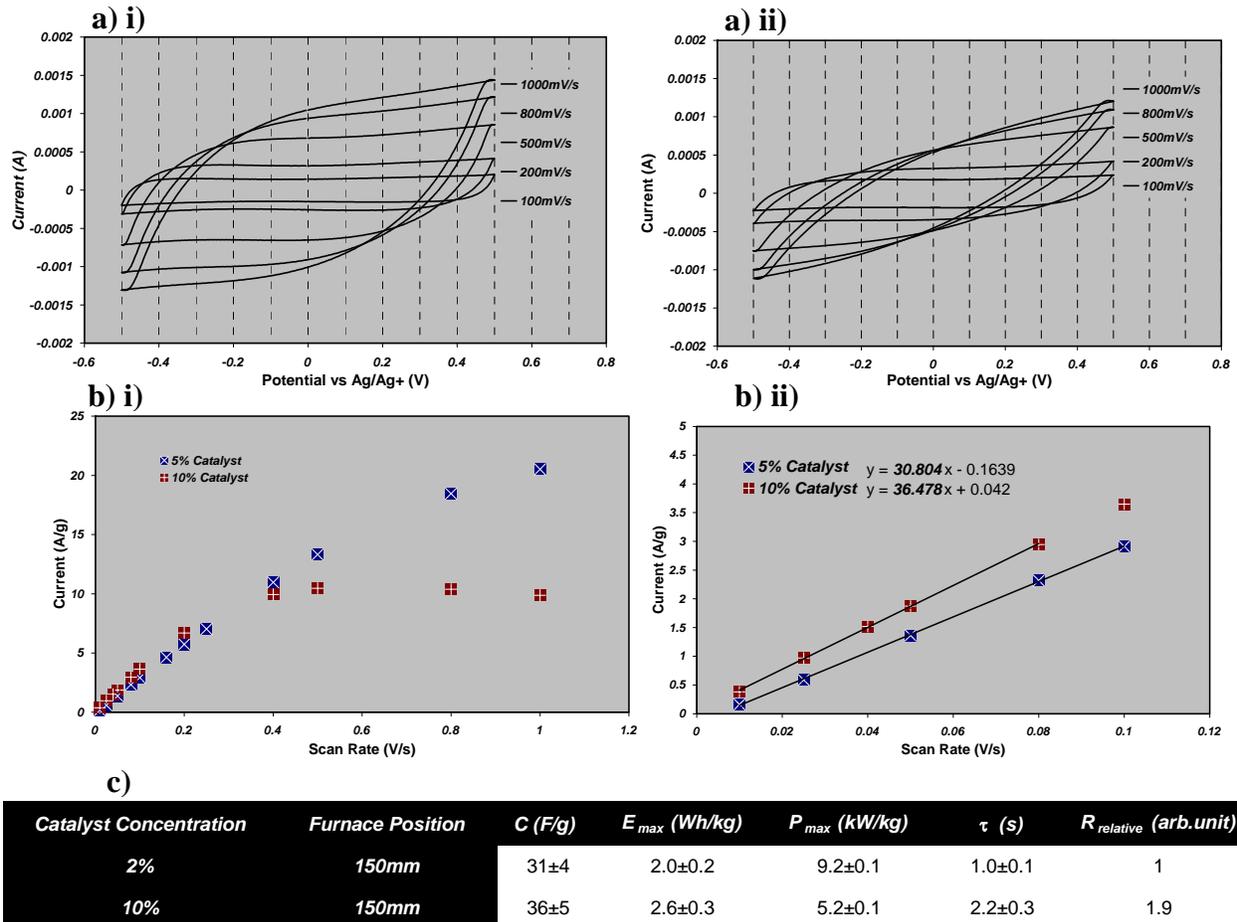
Initial work on the optimization of these architectures focused on a quantitative study of the effect of catalyst concentration and furnace position. Analysis of the resultant samples via SEM imaging (Figure 2) revealed a cross-dependence on these two variables. Specifically, for the 2% sample, the quality of growth was optimal at the earliest furnace position (150mm) whereas for the 10% sample the final zone (250mm) examined was at the optimal position. This position is defined by the emergence of long tubular structures in preference to significantly shorter carbon structures. This variation is explained by considering the roles of the mixture of $H_{2(g)}$ and $C_2H_{2(g)}$ flowing through the furnace. The hydrogen gas is required to activate the nanoparticles for growth, so the more H_2 which the slides are exposed to the more catalyst is available for the growth of CNTs. As such the samples in the earlier zone (150mm) have a greater proportion of activated catalysts than the later zones. The acetylene on the other hand decomposes to produce the carbon radicals which will interact with the activated catalysts,

however if no catalyst is available these radicals recombine to form amorphous carbon. As such early in the furnace, at the highest gas mixture concentration, there is a maximum amount of catalyst activated. At this position for the lower catalyst concentrations (2% and 5%) these active catalysts capture an optimal amount of carbon radicals. However for the 10% catalytic sample there are too many active sites capturing radicals not allowing for the formation of the desired tubular architectures. At positions further from the gas inlet (200mm and 250mm) there are less catalytic particles activated which appears to be optimal for the 10% catalyst slide. The decrease in particle activation is detrimental for the 2% catalyst slides as there are excess carbon radicals over these slides depositing undesired amorphous carbon and causing a loss of tubular definition in the samples.
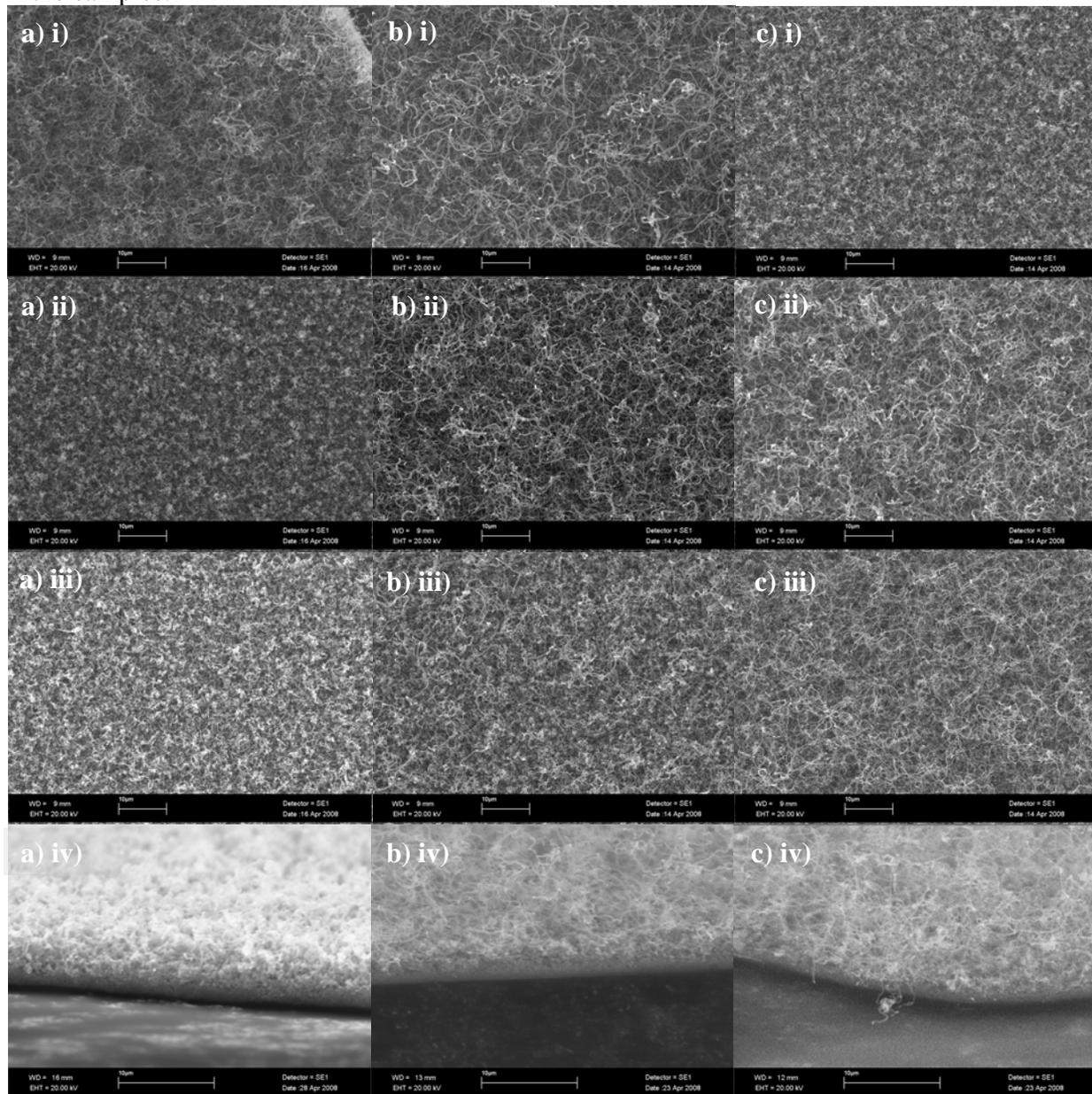
Figure 2. SEM images of eCNT network produced by varying the initial concentration of catalyst (Iron (III) Tosylate) **a)** 2%; **b)** 5%; and **c)** 10% and position from the gas source **i)** 150mm; **ii)** 200mm; and **iii-iv)** 250mm;

The variability in structures, induced by relatively minor changes in the growth conditions, is highlighted by the electrochemical performance of these electrodes. A simple capacitive analysis (Figure 3) reveals that there is a clear difference in stability between the 2% and 10% samples at 150mm. The 2% at150mm sample is stable at more than twice the scan rate of the equivalent 10% sample. This dramatic decrease arises from impedance of the TBAP ions moving through the sample, which in turn is induced by the loss of micro-porosity, observed in the previous micrographs, shown in Figure 3. Increased resistance within the composite system is evident from the CVs which is also reflected in the increase in the RC time constant. Despite this loss of ionic mobility at high scan rates it appears at slow scan rates that the capacitive response of the two materials is quite similar (Table 1), indicating the total available electro-active surface area is fundamentally similar for both samples.

Catalyst Concentration	Furnace Position	C (F/g)	E_{max} (Wh/kg)	P_{max} (kW/kg)	τ (s)	$R_{relative}$ (arb.unit)
2%	150mm	31±4	2.0±0.2	9.2±0.1	1.0±0.1	1
10%	150mm	36±5	2.6±0.3	5.2±0.1	2.2±0.3	1.9

Figure 3. Electrochemical analysis of entangled carbon architectures; **a)** cyclic voltammetry in 0.01M TBAP/ACN; **i)** 2% catalyst @ 150mm; **ii)** 10% @150mm; **b)** capacitance calculations; **i)** at the full range of scan rates; **ii)** within the full linear region at slower scan rates; and **c)** tabulated comparison of capacitive, energy and power densities determined from the cyclic voltammograms.

Deposition of conductive nanoparticles onto the highly porous structures allows for the tuning of these generic scaffolds towards specific applications whilst also increasing the available surface area. A microwave-assisted polyol reduction was developed for use on the eCNT architecture producing nanoparticles of sub 20nm for Gold, Palladium and Platinum. This method showed excellent deposition of nanoparticles onto the MWNTs (Figure 4) (only

Platinum nanoparticles shown). Figures 4a and 4b show the emergence of a peak at ≈37° in the XRD diffraction pattern corresponding to platinum deposition onto the composite structure. Photon correlation spectroscopy (Figure 4d) of the Au, Pd and Pt nanoparticle solutions confirmed the production of sub 20nm particles for Au and Pd, and sub 10nm particles were measured for the Pt samples.
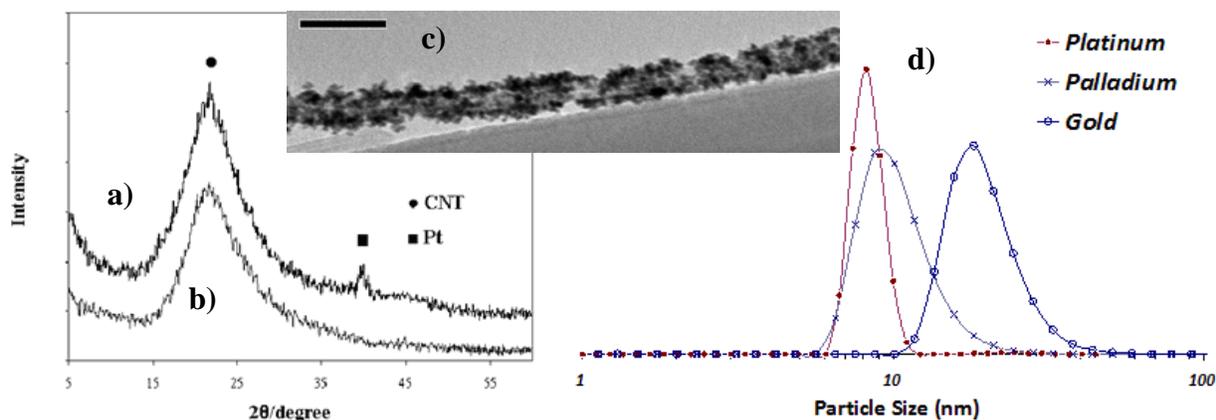
Figure 4. XRD spectra of **a)** NanoWeb architecture coated with platinum; and **b)** untreated NanoWeb architechture; **c)** TEM image of MWNT coated with Platinum nanoparticles (scale bar is 50nm); and **d)** photon correlation spectra for Platinum, Palladium and Gold nanoparticles.

The exceptional loading of Platinum nanoparticles observed arises due to the combination of intense heating of the CNTs causing localized metal reduction at the CNT/electrolyte interface and the concurrent formation of defect sites having dangling bonds which the particles can attach to. The effect of the deposition on the conductivity of the architectures is minimal with the resistance approximately 47±2 Ω/square. The variation in the capacitance of these electrodes, however, is extremely dramatic with the capacitance determined to be as high as 300±20 F/g.

CONCLUSIONS

The growth of 3D eCNT architectures via CVD is highly dependant on a number of variables. Furthermore these variables are not independent of one another, rather there is a clear interaction between these variables which must be accounted for before the ability to 'design' an electrode is attainable. The electrochemical response of the architectures is quite good at 36±F/g and very stable at scan rates up to 500mV/s. The addition of nanoparticles to the eCNT structure increased the electro-active surface area resulting in a 10fold increase in the pure capacitive response of these composite electrodes.

ACKNOWLEDGMENTS

REFERENCES

1. Kimizuka, O., et al., *Carbon,* 2008. **46(14)**: p. 1999-2001.
2. Bordjiba, T., M. Mohamedi, and L.H. Dao, *Journal of The Electrochemical Society*, 2008. **155(2)**: p. A115-A124.
3. Bordjiba, T., M. Mohamedi, and L.H. Dao, *Advanced Materials*, 2008. **20(4)**: p. 815-819.
4. Balasubramanian, K. and M. Burghard, *Journal of Materials Chemistry*, 2008. **18(26)**: p. 3071-3083.
5. Gooding, J.J., *Electrochimica Acta*, 2005. **50(15)**: p. 3049-3060.
6. Riccardis, M.F.D., et al., *Carbon*, 2006. **44(4)**: p. 671-674.
7. Sun, X., et al., *Chemical Physics Letters*, 2004. **394(4-6)**: p. 266-270.
8. Paradise, M. and T. Goswami, *Materials and Design*, 2007. **28(5)**: p. 1477-1489.
9. Chen, J., et al., *Advanced Materials*, 2008. **20(3)**: p. 566-570.
10. Chang, L. and C. Hui-Ming, J*ournal of Physics D: Applied Physics*, 2005. **(14)**: p. R231.
11. Thostenson, E.T., Z. Ren, and T.-W. Chou, *Composites Science and Technology*, 2001. **61(13)**: p. 1899-1912.
12. Kim, H.-T., J.-K. Lee, and J. Kim, *Journal of Power Sources*, 2008. **180(1)**: p. 191-194.
13. Wang, X., et al., *Journal of Power Sources*, 2006. **158(1)**: p. 154-159.
14. Raghuveer, M.S., et al., *Chem. Mater.*, 2006. **18(6)**: p. 1390-1393.
15. Bonet, F., et al., *Nanostructured Materials*, 1999. **11(8)**: p. 1277-1284.
16. Chen, W.-X., J.Y. Lee, and Z. Liu, *Materials Letters*, 2004. **58(25)**: p. 3166-3169.
17. Georgakilas, V., et al., *Journal of Materials Chemistry*, 2007. **17**: p. 2679-2694.
18. Zou, Y., et al., *Biosensors and Bioelectronics*, 2008. **23(7)**: p. 1010-1016.
19. He, Z., et al., *Diamond and Related Materials*, 2004. **13(10)**: p. 1764-1770.
20. Wang, Z.-C., et al., *Journal of Solid State Electrochemistry*, DOI: 10.1007/s10008-008-0558-7.
21. Chen, W., et al., *J. Am. Chem. Soc.*, 2006. **128(10)**: p. 3136-3137.